유전체가 입혀진 전자기 결합 동축 다이폴 어레이 안테나의 해석

Analysis of Dielectric Coated Electromagnetically Coupled Coaxial Dipole Array (ECCDA) Antenna

구 성 모*, 양 우 석*, 이 창 원**

Sung-Mo Koo*, Woo-Suk Yang*, Chang-Won Lee**

요 약

전자기 결합된 동축 다이폴 안테나를 이론적으로 해석하였다. 방사도파관 모드와 퓨리어 변환을 이용하여 적분 방정식을 유도하였다. 적분 방정식에 포함된 적분들을 빠르게 계산하기 위하여 실수축을 따른 적분을 브랜치 컷 (branch cut)을 따른 적분 경로로 변환 하여 계산 하였다. 방사 특성에 미치는 슬롯과 다이폴 그리고 단락면의 길이 그리고 유전체 코팅의 영향을 조사 하였다. 방시특성 또한 연구하였다. 제안된 방법의 타당성을 증명하기위하여 기존에 발표된 방법으로 계산한 안테나의 방향성 이득과 비교하였고 또한 전력 보존 법칙을 만족시키는지를 확인 하였다. 본 논문에서 제시한 방법으로 계산된 결과를 전자파 상용 시뮬레이터의 결과와 비교하여 잘 일치함을 확인 하였다.

ABSTRACT

Electromagnetically coupled coaxial dipole (ECCD) array antenna with and without short-ended termination is investigated theoretically. The integral equations are derived for the structure by use of the Fourier transform and mode expansion of radial waveguide. The integrals appearing in the integral equations are evaluated along the branch cut instead of real axis for a faster convergent integral. The effects of slots and dipoles, short-ended termination length, and dielectric coating on the radiation characteristics are presented. Radiation pattern of the structure is also investigated. The results of the present method are compared with those of the commercial EM simulator and good agreement is found.

Key words : Dipole antenna, coaxial collinear antenna, coaxial waveguide

Ⅰ. Introduction

The collinear antenna has been considered as an antenna element to replace two-dimensional dipole arrays because of the simple feeding structure. There are some kinds of collinear antennas; The coaxial collinear (COCO) antenna [1-3] is connected by interchanging the inner and outer conductors of the coaxial cable at each section made of a half-wavelength so as to produce in-phase and equal magnitude excitation voltages. Another type of the collinear antenna is the coaxial dipole antenna (CDA)

*School of Information and Communication · Media, Doowon Technical College
**School of Electrical Engineering and Computer Science, Kyungpook National University
접수 일자 : 2004. 7. 29 수정 완료 : 2004. 10. 20
논문 번호 : 2004-2-9
※본 연구는 두원공과대학 연구비 지원에 의해 수행되었음.

[4] fed by an annular ring slot of the feed coaxial cable which has much simpler feed structure when compared with that of COCO antennas.

Recently, the coaxial collinear antenna and slotted coaxial antenna were studied by using transmission line analysis to check the possibility of them as the base-station antenna for personal communication systems [5]. The electromagnetically coupled coaxial dipole (ECCD) [6] composed of a half-wavelength metallic circular pipe electromagnetically fed by an annular ring slot on the outer conductor of the feeding coaxial cable was analyzed as a kind of coaxial dipole antennas. In [6], the transmission line analysis with the input admittance of the dipole which calculated by use of the Wiener-Hopf technique is applied to analyze the array performance of the ECCD antenna. Therefore, in this study, the mutual coupling effect was not taken into account. A quarter wavelength impedance transformer is used for four-element array antenna impedance matching. This quarter wavelength impedance transformer gives the complexity of design. The radiation characteristics of dielectric-coated coaxial waveguide periodic slot was investigated in a viewpoint of leaky wave antenna [7].

In this paper, electromagnetically coupled coaxial dipole array antenna is investigated theoretically. The impedance matching is made without a quarter wavelength impedance transformer by controlling the length of the short-ended termination from the center of the last slot, which totally reflects the transmitted waves. The analysis and procedure are almost same as [7]. The fields in the slot region are expressed as summation of the radial waveguide TM modes and in other regions are expressed in the spectral domain by use of the inverse Fourier transformation. Boundary conditions at the interfaces are enforced and the simultaneous linear equations are derived [7,8]. Since the integrands of the integrals appearing in the linear equations contain the surface wave poles and branch points, the integral path can be deformed into a path along the branch cut. The reason for this deformation is to obtain a faster convergent integral, because the integrand decays exponentially along this deformed path. The slot electric fields and dipole electric currents are obtained by solving the simultaneous linear equations. The effects of slots and dipoles, short-ended termination length, and dielectric coating on the radiation characteristics are investigated.

II. Formulation

The geometry of the structure is shown in Fig. 1. It is assumed that the geometry is circular symmetry and the slots are excited by the dominant TEM mode of the coaxial waveguide. In region (I), the incident coaxial waveguide TEM mode is expressed

$$H_{\phi}^{i}(\rho,z)=\frac{V}{\ln(b/a)\eta_1}\frac{1}{\rho}e^{-jk_1 z} \tag{1}$$

where η_1 is the intrinsic impedance of the coaxial waveguide region. The scattering field in coaxial waveguide are expressed as, by use of the inverse Fourier transform with the equivalence principal,

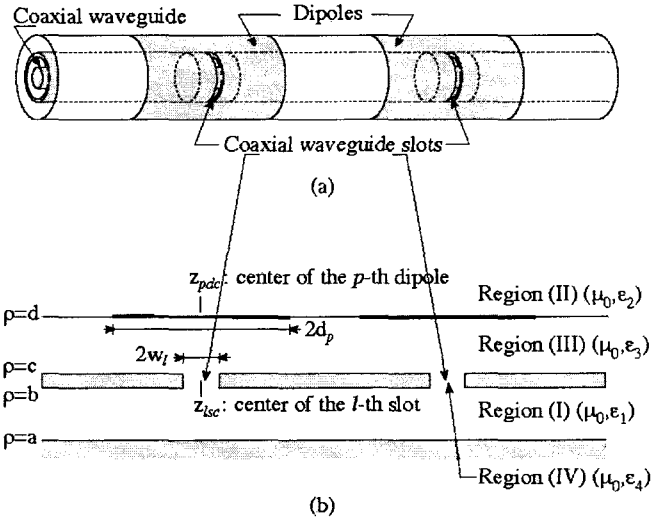

Fig. 1 Geometry of the problem

$$H_{\phi}^{s(1)}(\rho,z)=\frac{V}{\ln(b/a)\eta_1}\frac{1}{\rho}e^{-jk_1(2z_{sh}-z)}+\frac{1}{2\pi}\int_{-\infty}^{\infty}d\zeta e^{-j\zeta z}\tilde{H}_{\phi}^{s(1)}(\zeta)M_e(\zeta,\rho) \tag{2}$$

where

$$M_e(\zeta,\rho)=H_1^{(2)}(k_{\rho 1}\rho)-\frac{H_0^{(2)}(k_{\rho 1}a)}{H_0^{(1)}(k_{\rho 1}a)}H_1^{(1)}(k_{\rho 1}\rho)$$

$$k_{\rho 1}=\sqrt{k_1^2-\zeta^2}$$

and $H_n^{(1)}(\cdot)$ and $H_n^{(2)}(\cdot)$ are the n order Hankel function of the first and second kind, respectively. Here

the boundary conditions at the $\rho=a$ is already imposed. The vanishing condition of the tangential electric field at $z=z_{sh}$ can be imposed by introducing images of the slot electric fields with center of z_{sh}. Here the first term is corresponding to

the reflected TEM wave due to the short ended located at $z=z_{sh}$.

In region (II), The fields are expressed as a superposition of outgoing waves in the ρ-direction, by use of the inverse Fourier transform

$$H_{\phi}^{(II)}(\rho,z)=\frac{1}{2\pi}\int_{-\infty}^{\infty}d\zeta e^{-j\zeta z}\tilde{H}_{\phi(II)}(\zeta)H_1^{(2)}(k_{\rho 2}\rho) \tag{3}$$

where $k_{\rho 2}=\sqrt{k_2^2-\zeta^2}$.

The fields in region (III) are expressed as a superposition of outgoing and incoming waves (standing waves) in the ρ-direction

$$H_{\phi}^{(III)}(\rho,z)= \frac{1}{2\pi}\int_{-\infty}^{\infty}d\zeta e^{-j\zeta z}\left[\begin{matrix}\widetilde{H_{\phi}^{(III)+}}(\zeta)H_1^{(2)}(k_{\rho 3}\rho)\\ +\widetilde{H_{\phi}^{(III)-}}(\zeta)H_1^{(1)}(k_{\rho 3}\rho)\end{matrix}\right] \tag{4}$$

where $k_{\rho 3}=\sqrt{k_3^2-\zeta^2}$.

The fields in l-th slot satisfying the boundary condition at $z=z_{lsc}$ can be expressed in terms of radial waveguide TM modes

$$H_{\phi}^{(IV)}(\rho,z)=\sum_{m=0}^{\infty}\cos w_m^l(z+w_l-z_{lsc}) \times\left[b_m^l\frac{H_1^{(1)}(k_{\rho 4m}^l\rho)}{H_1^{(1)}(k_{\rho 4m}^l c)}+c_m^l\frac{H_1^{(2)}(k_{\rho 4m}^l\rho)}{H_1^{(2)}(k_{\rho 4m}^l b)}\right] \tag{5}$$

where $k_{\rho 4m}^l=\sqrt{k_4^2-w_m^{l\,2}}$ and $w_m^l=m\pi/2w_l$.

In the field expressions, there are 6 unknowns

$\tilde{H}_{\phi}^{s(I)}(\zeta)$, $\tilde{H}_{\phi(II)}(\zeta)$, $\tilde{H}_{\phi(III)+}(\zeta)$, $\tilde{H}_{\phi(III)-}(\zeta)$, b_m^l, and c_m^l to be determined. These unknowns can be determined by use of the boundary conditions. The boundary conditions will be imposed at the every interfaces and are given

$$E_z^{s(I)}(b,z)=\begin{cases}E_z^{(IV)}(b,z), & \text{on the slots}\\ 0, & \text{otherwise}\end{cases} \tag{6}$$

$$H_{\phi}^{i}(b,z)+H_{\phi}^{s(I)}(b,z)=H_{\phi}^{(IV)}(b,z), \quad \text{on the slots} \tag{7}$$

$$E_z^{(III)}(c,z)=\begin{cases}E_z^{(IV)}(c,z), & \text{on the slots}\\ 0, & \text{otherwise}\end{cases} \tag{8}$$

$$H_{\phi}^{(III)}(c,z)=H_{\phi}^{(IV)}(c,z), \quad \text{on the slots} \tag{9}$$

$$E_z^{(II)}(d,z)=E_z^{(III)}(d,z) \tag{10}$$

$$H_{\phi}^{(II)}(d,z)-H_{\phi}^{(III)}(d,z)=\begin{cases}J_z(z), & \text{on the dipoles}\\ 0, & \text{otherwise}\end{cases} \tag{11}$$

$$E_z^{(II)}(d,z)=0, \quad \text{on the dipoles} \tag{12}$$

where the unknown p-th dipole electric current $J_{zp}(z)$ is expanded as, by using sine function automatically zero at the end points

$$J_{zp}(z)=\sum_{v=1}^{\infty}J_{pv}\sin\alpha_v^p(z-z_{pdc}+d_p), \quad |z-z_{pdc}|\le d_p$$

where z_{pdc} and d_p are the center and half length of the

p-th dipole, respectively, and $\alpha_v^p=v\pi/2d_p$.

$\tilde{H}_{\phi(II)}(\zeta)$ can be expressed in terms of the radial waveguide TM mode by taking Fourier transform of the tangential electric field continuity condition (6) at $\rho=b$. After imposing the remained boundary conditions (7-11), we can express the spectrum amplitudes in terms of the equivalent slot magnetic current and dipole electric surface current. Using the results of the above spectrum amplitudes, we have following integral equations

$$\frac{V}{\ln(b/a)\eta_1 b}\left[Q_r^n(-k_1)+Q_r^n(k_1)e^{-j2k_{1z_{sh}}}\right] +\sum_l\sum_m\frac{\epsilon_1 k_{\rho 4m}^l}{2\pi\epsilon_4}\left[b_m^l\frac{H_0^{(1)}(k_{\rho 4m}^l b)}{H_1^{(1)}(k_{\rho 4m}^l c)}+c_m^l\frac{H_0^{(2)}(k_{\rho 4m}^l b)}{H_1^{(2)}(k_{\rho 4m}^l b)}\right]I_{1,rl}^{nm} =\alpha_n w_r\left[b_n^r\frac{H_1^{(1)}(k_{\rho 4n}^r b)}{H_1^{(1)}(k_{\rho 4n}^r c)}+c_n^r\right] \tag{13}$$

$$\sum_l\sum_m\frac{\epsilon_{r3}k_{\rho 4m}^l}{2\pi\epsilon_{r4}}\left[b_m^l\frac{H_0^{(1)}(k_{\rho 4m}^l c)}{H_1^{(1)}(k_{\rho 4m}^l c)}+c_m^l\frac{H_0^{(2)}(k_{\rho 4m}^l c)}{H_1^{(2)}(k_{\rho 4m}^l b)}\right]I_{2,rl}^{nm} +\sum_p\sum_v\tilde{J}_{pv}\frac{2\epsilon_{r3}}{j\pi^2 c}I_{3,rp}^{nv}=\left[b_n^r+c_n^r\frac{H_1^{(2)}(k_{\rho 4n}^r c)}{H_1^{(2)}(k_{\rho 4n}^r b)}\right]\alpha_n w_r \tag{14}$$

$$\sum_l\sum_m\frac{k_{\rho 4m}^l}{\epsilon_{r4}}\left[b_m^l\frac{H_0^{(1)}(k_{\rho 4m}^l c)}{H_1^{(1)}(k_{\rho 4m}^l c)}+c_m^l\frac{H_0^{(2)}(k_{\rho 4m}^l c)}{H_1^{(2)}(k_{\rho 4m}^l b)}\right]\frac{2j\epsilon_{r3}}{\pi^2 d}I_{4,ql}^{um} +\sum_p\sum_v\tilde{J}_{pv}\frac{1}{2\pi}I_{5,qp}^{uv}=0 \tag{15}$$

where

$$I_{2,rl}^{nm}=\int_{-\infty}^{\infty}d\zeta\frac{N_{h(\zeta)}}{k_{\rho 3}N_e(\zeta)}Q_l^{m(\zeta)}Q_r^n(-\zeta)$$

$$I^{nv}_{3,rp}=\int_{-\infty}^{\infty}d\zeta\frac{k_{\rho 2}H_0^{(2)}(k_{\rho 2}d)}{k_{\rho 3}R_D(\zeta)N_e(\zeta)}S_p^v(\zeta)Q_r^n(-\zeta)$$

$$I^{um}_{4,ql}=\int_{-\infty}^{\infty}d\zeta\frac{k_{\rho 2}H_0^{(2)}(k_{\rho 2}d)}{k_{\rho 3}R_D(\zeta)N_e(\zeta)}Q_l^m(\zeta)S_q^u(-\zeta)$$

$$I^{uv}_{5,qp}=\int_{-\infty}^{\infty}d\zeta\frac{k_{\rho 2}k_{\rho 3}H_0^{(2)}(k_{\rho 2}d)N_j(\zeta)}{R_D(\zeta)N_{e(\zeta)}}S_p^v(\zeta)S_q^u(-\zeta)$$

and

$$M_e(\zeta)=H_0^{(2)}(k_{\rho 1}b)-\frac{H_0^{(2)}(k_{\rho 1}a)}{H_0^{(1)}(k_{\rho 1}a)}H_0^{(1)}(k_{\rho 1}b)$$

$$M_h(\zeta)=H_1^{(2)}(k_{\rho 1}b)-\frac{H_0^{(2)}(k_{\rho 1}a)}{H_0^{(1)}(k_{\rho 1}a)}H_1^{(1)}(k_{\rho 1}b)$$

$$N_{h(\zeta)}=H_1^{(2)}(k_{\rho 3}c)+R(\zeta)H_1^{(1)}(k_{\rho 3}c)$$

$$N_{e(\zeta)}=H_0^{(2)}(k_{\rho 3}c)+R(\zeta)H_0^{(1)}(k_{\rho 3}c)$$

$$R(\zeta)=-\frac{\epsilon_2k_{\rho 3}H_1^{(2)}(k_{\rho 2}d)H_0^{(2)}(k_{\rho 3}d)-\epsilon_3k_{\rho 2}H_0^{(2)}(k_{\rho 2}d)H_1^{(2)}(k_{\rho 3}d)}{\epsilon_2k_{\rho 3}H_1^{(2)}(k_{\rho 2}d)H_0^{(1)}(k_{\rho 3}d)-\epsilon_3k_{\rho 2}H_0^{(2)}(k_{\rho 2}d)H_1^{(1)}(k_{\rho 3}d)}=\frac{R_N(\zeta)}{R_D(\zeta)}$$

$$T(\zeta)=\frac{\epsilon_2 4j/(\pi d)}{\epsilon_2k_{\rho 3}H_1^{(2)}(k_{\rho 2}d)H_0^{(1)}(k_{\rho 3}d)-\epsilon_3k_{\rho 2}H_0^{(2)}(k_{\rho 2}d)H_1^{(1)}(k_{\rho 3}d)}$$

$$S_p^v(\zeta)=\frac{a_v^p[e^{j\zeta d_p}(-1)^v-e^{-j\zeta d_p}]e^{j\zeta z_{pdc}}}{\zeta^2-a_v^{p\,2}}$$

$$Q_l^m(\zeta)=\frac{-j\zeta[e^{j\zeta w_l}(-1)^m-e^{-j\zeta w_l}]e^{j\zeta z_{bc}}}{\zeta^2-w_m^{l\,2}}$$

$$a_n=\begin{cases}2, & n=0\\ 1, & n\neq 0\end{cases}.$$

Using above integral equations (13), (14), and (15), we have following simultaneous linear equations

$$\begin{bmatrix}\Psi_1 & \Psi_2 & 0\\ \Psi_3 & \Psi_4 & \Psi_5\\ \Psi_6 & \Psi_7 & \Psi_8\end{bmatrix}\begin{bmatrix}B\\ C\\ J\end{bmatrix}=\begin{bmatrix}S\\ 0\\ 0\end{bmatrix}\qquad(16)$$

where

$$\Psi_{1,rl^{nm}}=\frac{\varepsilon_{r1}k^l_{\rho 4m}}{2\pi\varepsilon_{r4}}\frac{H_0^{(1)}(k^l_{\rho 4m}b)}{H_1^{(1)}(k^l_{\rho 4m}c)}I^{nm}_{1,rl}-a_nw_r\frac{H_1^{(1)}(k^r_{\rho 4n}b)}{H_1^{(1)}(k^r_{\rho 4n}c)}\delta_{rl}\delta_{nm}$$

$$\Psi_{2,rl^{nm}}=\frac{\varepsilon_{r1}k^l_{\rho 4m}}{2\pi\varepsilon_{r4}}\frac{H_0^{(2)}(k^l_{\rho 4m}b)}{H_1^{(2)}(k^l_{\rho 4m}b)}I^{nm}_{1,rl}-a_nw_r\delta_{rl}\delta_{nm}$$

$$\Psi_{3,rl^{nm}}=\frac{\varepsilon_{r3}k^l_{\rho 4m}}{2\pi\varepsilon_{r4}}\frac{H_0^{(1)}(k^l_{\rho 4m}c)}{H_1^{(1)}(k^l_{\rho 4m}c)}I^{nm}_{2,rl}-a_nw_r\delta_{rl}\delta_{nm}$$

$$\Psi_{4,rl^{nm}}=\frac{\varepsilon_{r3}k^l_{\rho 4m}}{2\pi\varepsilon_{r4}}\frac{H_0^{(2)}(k^l_{\rho 4m}c)}{H_1^{(2)}(k^l_{\rho 4m}b)}I^{nm}_{2,rl}-a_nw_r\frac{H_1^{(2)}(k^r_{\rho 4n}c)}{H_1^{(2)}(k^r_{\rho 4n}b)}\delta_{rl}\delta_{nm}$$

$$\Psi_{5,rp^{nv}}=\frac{2\varepsilon_{r3}}{j\pi^2c}I^{nv}_{3,rp}$$

$$\Psi_{6,ql^{um}}=\frac{k^l_{\rho 4m}}{\varepsilon_{r4}}\frac{H_0^{(1)}(k^l_{\rho 4m}c)}{H_1^{(1)}(k^l_{\rho 4m}c)}\frac{2j\varepsilon_{r3}}{\pi^2d}I^{um}_{4,ql}$$

$$\Psi_{7,ql^{um}}=\frac{k^l_{\rho 4m}}{\varepsilon_{r4}}\frac{H_0^{(2)}(k^l_{\rho 4m}c)}{H_1^{(2)}(k^l_{\rho 4m}b)}\frac{2j\varepsilon_{r3}}{\pi^2d}I^{um}_{4,ql}$$

$$\Psi_{8,qp^{uv}}=12\pi I^{uv}_{5,qp}$$

$$S_{r^n}=-\frac{V}{\ln(b/a)\pi_1b}[Q_r^n(-k_1)+Q_r^n(k_1)e^{-j2k_1z_{sh}}]$$

Since the integrand of $I^{nm}_{1,rl}$ contains the poles which correspond to the coaxial waveguide TM modes, the integral can be evaluated in a functional form by use of Cauchy residue theorem and is given in [7]. Because the integrands of $I^{nm}_{2,rl}$, $I^{nv}_{3,rp}$, $I^{um}_{4,ql}$, and $I^{uv}_{5,qp}$ have the surface wave poles and branch points, the integral path can be deformed into a path along the branch cut. The reason for this deformation is to obtain a faster convergent integral. The integral $I^{nm}_{2,rl}$ is given in [7] and the other integrals can be evaluated in the same manner described in [7].

Once the unknown radial waveguide mode coefficients (b_m^l and c_m^l) and dipole electric currents are determined by solving (16), $\mathcal{H}_{\phi(\mathrm{I})}(\zeta)$, $\mathcal{H}_{\phi(\mathrm{III})+}(\zeta)$, $\mathcal{H}_{\phi(\mathrm{III})-}(\zeta)$, and $\mathcal{H}_{\phi(\mathrm{II})}(\zeta)$ are computed by using the boundary conditions. Hence, all the field coefficients are known, the fields in each region can be calculated by use of the field equations. The wave radiated from slots and dipoles are divided into two wave types, i.e., one is the space wave which is radiated into the region (II), and the other the surface wave which is trapped in and above the dielectric and guided in the $\pm z$ directions. The far-zone magnetic field radiated into the region (II), by using an asymptotic evaluation and the surface wave in each region is calculated by applying the Cauchy residue theorem on the inverse Fourier transformation [7].

Part of the radiation power P_{rad} through the slots goes into the surface wave guided by the dielectric over the conductor and the balance into space wave. This part is carried in the surface wave is designated P_{surf}, while the part in the space wave is denoted P_{space}. The integral appearing in the calculation of the surface wave power can be expressed in a closed form by using the surface wave orthogonality property in the cylindrical coordinates given in [8].

III. Numerical Results and Discussions

Fig. 2. shows S_{11} and S_{12} versus the normalized frequency for a single dipole with short-ended termination removed and matched with the impedance of a coaxial waveguide (infinitely long coaxial waveguide). The parameters are $a=0.0026\lambda_{f_0}$, $b=0.0085\lambda_{f_0}$, $c=0.0092\lambda_{f_0}$, $d=0.0355\lambda_{f_0}$, $\varepsilon_{r1}=\varepsilon_{r3}=\varepsilon_{r4}=2.0$, $w=0.005\lambda_{f_0}$, $d=0.175\lambda_{f_0}$, and $z_{sc}=z_{dc}=0$, where λ_{f_0} corresponds to the free-space wavelength at the frequency f_0.

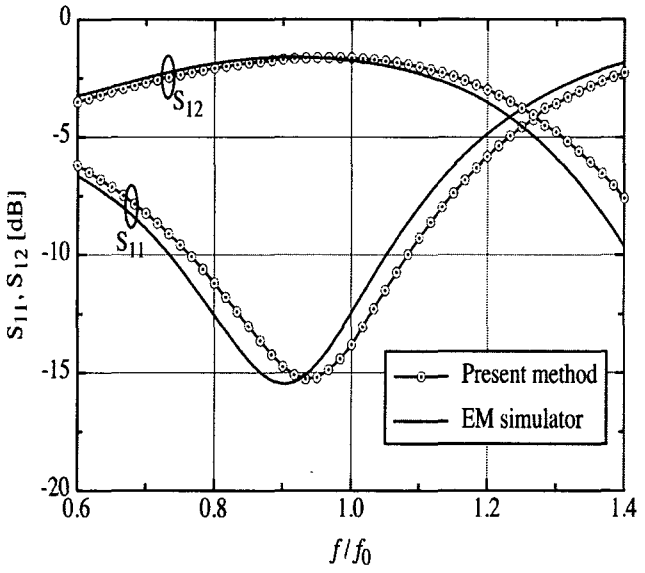

Fig. 2. Comparison between the present method and EM simulator values for S_{11} and S_{12} when the short-ended termination removed and terminated with matched load.

In order to verify the present method, the results of the commercial EM simulator are compared with those of the present method and also plotted in Fig. 3. In this figure, the results of the present method are very well matched with those of the EM simulator. When the EM simulator is performed, the infinitely long geometry along z-direction is modeled with $2\lambda_{f_0}$ finite long one center with slot center (or dipole center).

The normalized impedance of the equivalent circuit of Fig. 2. can be calculated from the reflected magnetic field in the region (I) [9] and plotted in Fig. 3. In this figure, the reactance (X) of the series equivalent impedance (Z) goes to zero around $f\simeq 0.93f_0$ and at this point resistance is almost $R\simeq 0.43$. Around this frequency, the return loss has its minimum value.

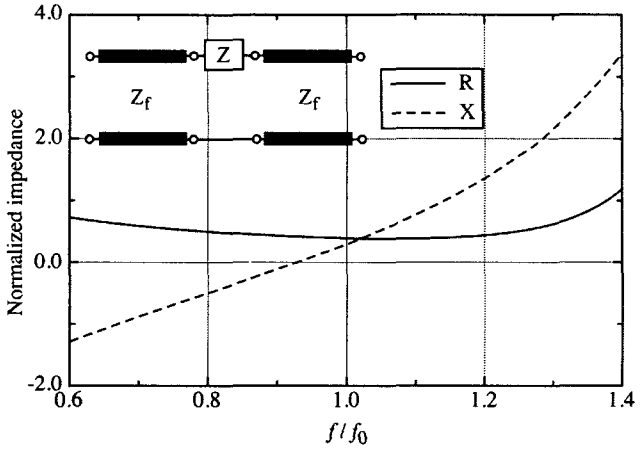

Fig. 3. The normalized series impedance of the equivalent circuit.

The validity of the numerical results in this study is assured by a check of the power conservation law:

$$P_{inc}=P_{ref}+P_{trans}+P_{rad}$$
$$P_{rad}=P_{space}+P_{surf}$$

The normalized powers of the single dipole are shown in Fig. 4. This figure shows that the power conservation law is satisfied for all frequencies. The surface wave power is larger than the space wave power to $f=0.87f_0$, but it is reversed as the operating frequencies increase. For $f=f_0$, 27.3% of the incident power is radiated into regions (II) and (III), 4.2% is reflected, and 68.5% is transmitted to the guide beyond the slotted region. 64.9% and 35.1% of the radiated power from the slots and dipoles into region (II) and (III) are launched into space and surface wave powers, respectively.

Fig. 5. shows the S_{11} versus the normalized frequency for a single dipole with short-ended termination located at $z_{sh}=0.38\lambda_g$, where $\lambda_g=\lambda_{f_0}/\sqrt{\varepsilon_{r1}}$. In this figure, the result of the presented method is very well matched with that of the EM simulator. The short-ended termination effects on the imaginary part of the input impedance of the structure. Thus, the minimum return loss frequency is shifted to $f\approx 1.07f_0$. This can be expected by calculating the series equivalent slot impedance of the structure in Fig. 3 and comparing the imaginary part of that with the input impedance of the short-ended termination at the slot center, i.e., $j\tan(k_1 z_{sh})$.

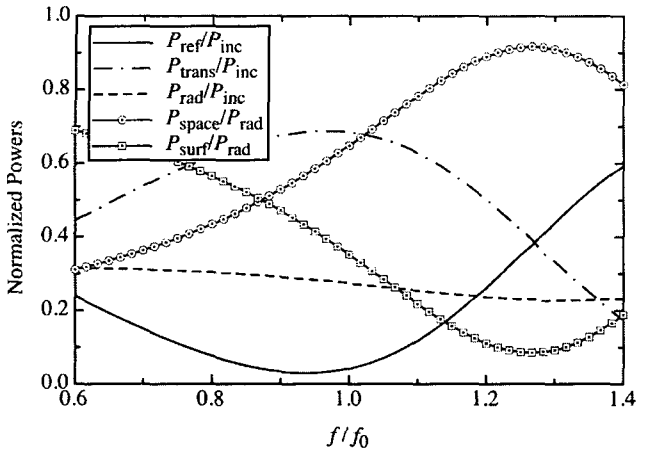

Fig. 4. Normalized powers P_{ref}, P_{trans}, P_{rad}, P_{space}, and P_{surf} versus normalized frequency. where the parameters are the same as those in Fig.2.

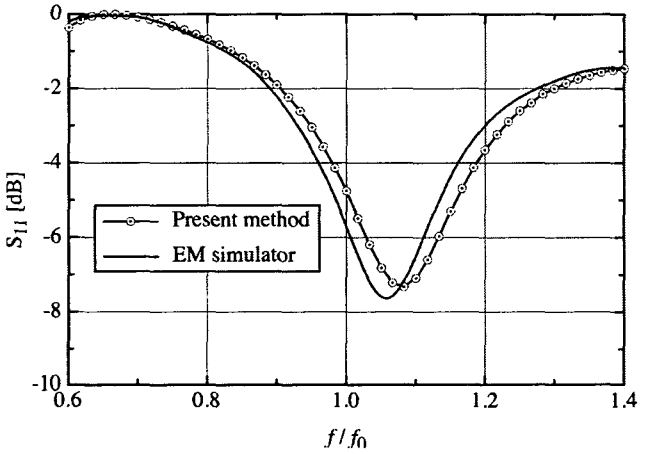

Fig. 5. Comparison between the present method and EM simulator values for S_{11} when the short end is located at $z_{sh}=0.38\lambda_g$

A four-element array antenna is designed. The parameters of the radiating elements are all identical to those of Fig. 5. The space of the radiating elements are all identical to $1.0\lambda_{f_0}$. The return loss of the four-element array antenna is shown in Fig. 6. This figure shows that the antenna is matched at frequencies $f=f_0$ and $f=1.1f_0$. The effect of the length between the short-ended termination and center of the last slot on the return loss is shown in Fig. 7. It is seen that the return loss is periodic with $\lambda_g/2$ periodicity, as expected from a transmission line theory. Therefore, the length between the short-ended termination and center of the last slot was chosen $0.38\lambda_g$ in the design of a four-element array antenna without a quarter wavelength impedance transformer. This gives more simplicity of design. Fig. 8 shows the slot electric field and dipole electric current distributions of the proposed array antenna. Slot electric fields and dipole electric currents are satisfying the edge conditions: the electric fields blow up as approaches to the slot edges and dipole electric currents go to zero at the dipole edges. The dipole currents are almost in-phase and uniform as expected in collinear antennas.

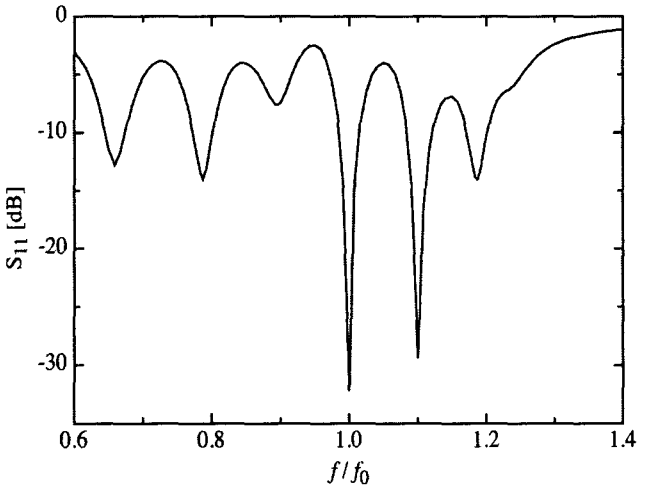

Fig. 6. The return loss of a four-element array antenna.

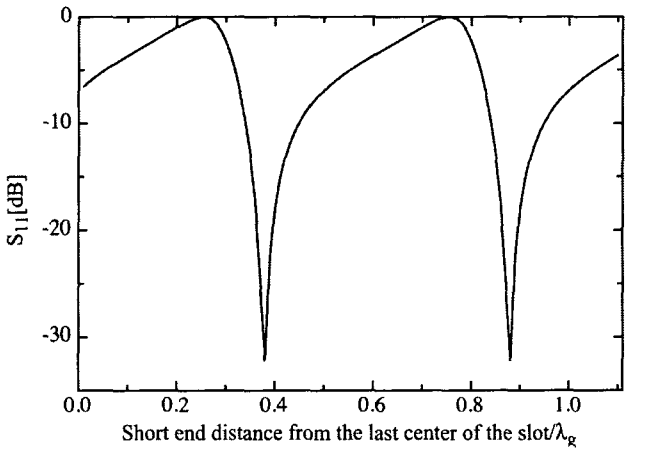

Fig. 7. The return loss versus short-ended termination distance.

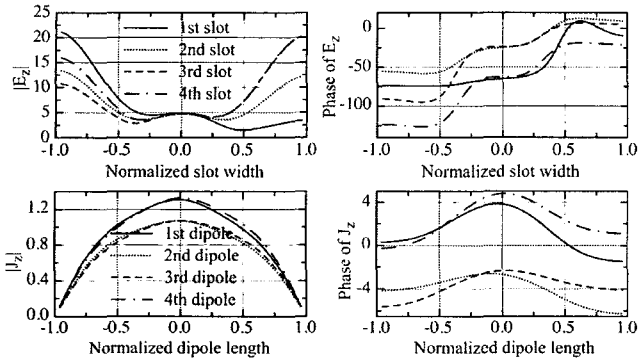

Fig. 8. Slot electric field and dipole electric current distributions of the proposed four-element array antenna.

To investigate the efficiency of the antenna, the surface and space wave powers of the designed four-element array antenna are calculated and plotted in Fig. 9. It is seen that the 99.3% and 0.7% of the radiated power from the slots and dipoles into region (II) and (III) are launched into space and surface wave powers at the first resonant frequency $f=f_0$, respectively. Thus, most of the coupled power in region (II) and (III) is radiated into region (II) as a space wave and the surface wave is negligible. This means that the undesired power loss by the surface wave due to the dielectric coating can be ignored for this four-element array antenna structure. Therefore, the dielectric coating has almost no effect on the antenna efficiency (P_{space}/P_{inc}) due to surface wave. The radiation efficiency of the antenna is 99.2%. But, at the second resonant frequency $f=1.1f_0$, 59.3% and 40.7% of the radiated power from the slots and dipoles are launched into space and surface wave powers, respectively. Therefore, the radiation efficiency of the antenna at the second resonant frequency is only 59.2%. This means that the undesired power loss by the surface wave due to the dielectric coating cannot be ignored at the frequency $f=1.1f_0$.

Fig. 10. shows the radiation pattern of the four-element array antenna at the frequency $f=f_0$. The side-lobe level and half beamwidth are -9.59[dB] and 17.3o, respectively. The directivity gain is 7.4[dB]. The validity of the proposed four-element array antenna is also checked by the approximate relationship between directivity and beamwidth for broadside collinear arrays [4,10], the approximately calculated directivity gain is 7.87[dB]. The value calculated by the proposed method is almost same with that obtained by an approximate method.

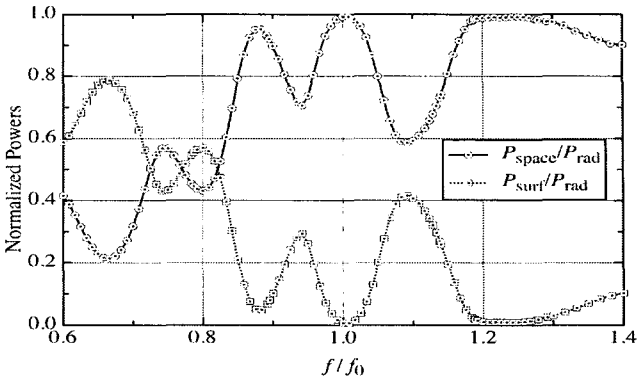

Fig. 9. Normalized powers P_{space} and P_{surf} versus normalized frequency.

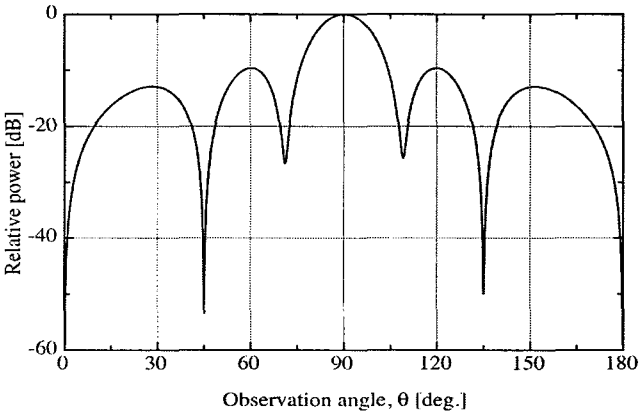

Fig. 10. The radiation pattern of a four-element array antenna.

Ⅳ. Conclusions

The analysis method for electromagnetically coupled coaxial dipole (ECCD) array antenna with and without short-ended termination is proposed. In this paper, rigorous mode matching technique and an integral equation formulation are applied. The validity of the proposed method is checked by all eying the power conservation law and comparing antenna directivity gain with that obtained by an approximate method. A good agreement between the results of the present method and those of the commercial EM simulator has been found. This also assures the validity of the proposed method. The four-element array antenna without having a quarter wavelength impedance transformer is designed by controlling the location of the short-ended termination. The undesired power loss by the surface wave due to the dielectric coating can be avoided by carefully chosen parameters of the structure.

It is thought that the proposed antenna can be applied to the base-station antenna, the surveillance radar for air traffic control or the omnidirectional antenna for the telemetry, command and ranging (TC & R) subsystem of communication satellite.

References

[1] T. J. Judasz, W. L. Ecklund, and B. B. Balsley, "The coaxial collinear antenna: Current distribution from the cylindrical antenna equation," IEEE Trans. Antennas Propagat., vol. AP-35, no. 3, pp. 327-331, Mar. 1989

[2] T. J. Judasz and B. B. Balsley, "Improved theoretical and experimental models for the coaxial collinear antenna," IEEE Trans. Antennas Propagat., vol. AP-37, no. 3, pp. 289-296, Mar. 1989

[3] A. Sakitani and S. Egashira, "Analysis of coaxial collinear antenna: Recurrence formula of voltages and admittances at connections," IEEE Trans. Antennas Propagat., vol. AP-39, no. 1, pp. 15-20, Jan. 1991

[4] P. Volta, "Design and development of an omnidirectional antenna with collinear array of slots," Microwave J., vol. 25, no. 12, pp. 111-115, 1982

[5] Jean-Fu Kiang, "Analysis of linear coaxial antennas," IEEE Trans. Antennas Propagat., vol. AP-46, no. 5, pp. 636-642, May 1998

[6] H. Miyashita, H. Ohmine, K. Nishizawa, S. Makino, and S. Urasaki, "Electromagnetically coupled coaxial dipole array antenna," IEEE Trans. Antennas Propagat., vol. AP-47, no. 11, pp. 1716-1726, Nov. 1999

[7] C. W. Lee and H. Son, "Radiation characteristics of dielectric-coated coaxial waveguide periodic slot with finite and zero thickness," IEEE Trans. Antennas Propagat., vol. AP-47, no. 1, pp. 16-25, Jan. 1999

[8] C. W. Lee and J. P. Kim, "Radiation characteristics of corrugation loaded dielectric-coated conducting cylinder," IEEE Trans. Antennas Propagat., vol. AP-51, no. 6, pp. 1321-1330, June 2003

[9] C. W. Lee and H. Son, "Periodically slotted dielectrically filled parallel-plate waveguide as a leaky-wave antenna: E-polarization case," IEEE Trans. Antennas Propagat., vol. AP-47, no. 1, pp. 171-178, Jan. 1999

[10] N. A. McDonald, "Approximate relationships between directivity and beamwidth for broadside collinear arrays," IEEE Trans. Antennas Propagat., vol. AP-26, no. 2, pp. 340-341, Mar. 1978

Sung-Mo Koo

He received the B.S., M.S., and Ph. D. degrees in electronics engineering from Kyungpook National University, Daegu, Korea, in 1987, 1993, and 1998, respectively.

Since 1995, he has been a Professor at School of Information and Communication · Media, Doowon Technical College, Kyonggido, Korea. His current research interests include analytical and numerical solutions to electromagnetic radiation and scattering problems, bioelectromagnetics. biomedical image processing and hyperthermia

Chang-Won Lee

He received the B.S., M.S., and Ph. D. degrees in electronics engineering from Kyungpook National University, Daegu, Korea, in 1991, 1993, and 1998, respectively.

From 1999 to 2000, he was a Postdoctoral Research Associate at the Center for Computational Electromagentics, Department of Electrical and Computer Engineering, University of Illinois Urbana-Champaign. Since 2001, he has been a Contract Professor at School of Electrical Engineering and Computer Science, Kyungpook National University, Daegu, Korea. His current research interests include analytical and numerical solutions to electromagnetic radiation and scattering problems, printed antennas, periodic structures and bioelectromagnetics.

Dr. Lee received an URSI Commission B Young Scientist Award in the 1995 Electromagnetic Theory Symposium, St. Petersburg, Russia.

Woo-Suk Yang

He received the B.S., M.S., and Ph. D. degrees in electronics engineering from Kwangwon University, Seoul Korea, in 1985, 1989, and 1998, respectively.

Since 2002, he has been a Professor at School of Information and Communication · Media, Doowon Technical College, Kyonggido, Korea. His current research interests include analytical and numerical solutions to electromagnetic radiation and scattering problems, satellite and wireless communications, traffic and protocol analysis of internetworking.